



**HAL**  
open science

# Characterization of the turbulent bi-stable flow regime of a 2D bluff body wake disturbed by a small control cylinder

Vladimir Parezanovic, Romain Monchaux, Olivier Cadot

► **To cite this version:**

Vladimir Parezanovic, Romain Monchaux, Olivier Cadot. Characterization of the turbulent bi-stable flow regime of a 2D bluff body wake disturbed by a small control cylinder. *Experiments in Fluids*, 2015, 56(1) (12), pp.1-8. 10.1007/s00348-014-1890-6 . hal-01168640

**HAL Id: hal-01168640**

**<https://ensta-paris.hal.science/hal-01168640v1>**

Submitted on 26 Jun 2015

**HAL** is a multi-disciplinary open access archive for the deposit and dissemination of scientific research documents, whether they are published or not. The documents may come from teaching and research institutions in France or abroad, or from public or private research centers.

L'archive ouverte pluridisciplinaire **HAL**, est destinée au dépôt et à la diffusion de documents scientifiques de niveau recherche, publiés ou non, émanant des établissements d'enseignement et de recherche français ou étrangers, des laboratoires publics ou privés.

# Characterization of the turbulent bi-stable flow regime of a $2D$ bluff body wake disturbed by a small control cylinder

Vladimir Parezanović · Romain Monchaux · Olivier Cadot

DRAFT version August 18, 2014 14:07

**Abstract** A small control cylinder is placed in a turbulent wake of a  $2D$  bluff body in an effort to control such global features as the drag and the vortex shedding frequency. For certain positions of the control cylinder, large increase of drag fluctuations are recorded. Ensemble averages of PIV acquisitions and pressure measurements at the base of the bluff body reveal a bi-stable wake regime. Long duration hot-wire measurements are used to characterize the states and the transition process. The results show that a stochastic process is responsible for the transitions between the two stable states.

**Keywords** Turbulent wake · Steady perturbation · Bi-stable flow · Kármán vortex street

## 1 Introduction

In some geometric configurations of bluff cylinders a bi-stable wake flow can occur, where the flow switches between two distinct observable (stable) states. This situation creates large force fluctuations which are generally undesirable. Very often, its origin is related to the intermittent re-attachment of a separated boundary layer, where the two stable flows correspond either to the detached or attached boundary layer configuration. Commonly, bi-stability is observed in the case of

tandem arrangement of bluff bodies of equivalent sizes [1–5], but also using disturbances technique on a single body. A span-wise strip control wire positioned on the surface of a circular cylinder in the sub-critical regime can lead to a bi-stable behavior of the wake [6, 7]. In that case the disturbed separated boundary layers is either reattached or not on the base of the circular cylinder. Bi-stable flows were also observed when a small control cylinder is placed in the bulk of the flow [8–11]. The interesting effect is that the re-attachment occurring on the small control cylinder creates large force fluctuations on the primary (and much larger) body. This was first evidenced by [8] where large force fluctuations on the primary square prism were observed for some critical positions of the control circular cylinder in its wake. This behavior is characteristic to large Reynolds number flows, since such bi-stability was not observed in the laminar experiment of [12]. In [10], the methodical mapping of the wake revealed some critical locations for a "D" shaped cylinder, where large base pressure fluctuations were caused by the presence of the small control cylinder. In the sensitivity maps of mean drag and drag fluctuations, these positions correspond to the end of the influence zone of the control cylinder for drag reduction. The present article aims to explore the flow dynamics when the control cylinder is located in these critical regions. What are the two flow states? How do they switch from one to the other? We will use PIV measurements and long time acquisition of local velocity by hot-wire to characterize their spatial and statistical properties.

---

Vladimir Parezanović  
Institute PPrime, CNRS UPR3346, 43 Rue de l'Aerodrome,  
F-86000 Poitiers, France  
E-mail: vladimir.parezanovic@univ-poitiers.fr

R. Monchaux · O. Cadot  
Unité de Mécanique, Ecole Nationale Supérieure de Tech-  
niques Avancées - ParisTech, 828 Boulevard des Maréchaux,  
F-91762 Palaiseau Cedex, France

## 2 Experimental setup, measurements and post-processing

The test facility is an Eiffel type wind tunnel with less than 0.3% of turbulence intensity, and velocity homogeneity of 0.4%. The test section has a square cross-section of  $400\text{mm} \times 400\text{mm}$ , with open sides. Its length, from the inlet to the outlet, is 960mm. The primary cylinder is a "D" shaped bluff body (as depicted in figure 1); it has a semi-circular leading edge which continues into a rectangular aft section, for a combined length of  $2D = 50\text{mm}$ . The diameter of the semi-circle, and thus the height of the main cylinder, is  $D = 25\text{mm}$ . The span of the body is  $S = 600\text{mm}$ . The smaller control cylinder has a circular cross section and a diameter of  $d = 1, 2, 3$  or  $4\text{mm}$ . It has a span of 800mm and is sufficiently stretched on the support frame in order to avoid any flow-induced vibrations. The frame is connected to three *Newport (M-)MTM* long travel consoles, which are controlled by the *Newport Motion Controller ESP301*. Using the displacement consoles we are able to move the control cylinder to cover the entire area of the wake shown as the shaded rectangle in figure 1. The control cylinder is displaced with the accuracy better than 0.1mm. The Reynolds number of the flow  $\text{Re} = 13000$  is based on the height of the bluff body  $D = 25\text{mm}$  and the wind tunnel inlet velocity of  $U_0 = 8\text{m}\cdot\text{s}^{-1}$ . For more details on the facility and the mapping experiments we kindly refer the reader to our previous works [10, 11].

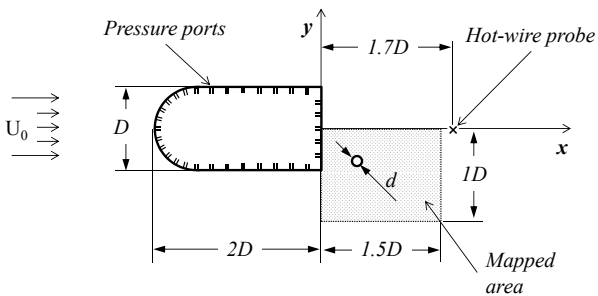


**Fig. 1** Sketch of the bluff body and the small control cylinder ( $D = 25\text{mm}$ , and  $d = 1, 2, 3$  or  $4\text{mm}$ ). Shaded area depicts the mapped portion of the wake.

The pressure is measured with 32 pressure taps distributed along the entire perimeter of the "D" cylinder cross-section at mid-span (figure 1). The taps are connected via plastic tubes of diameter  $\phi = 3\text{mm}$  and length of 1.5m to two *Scanivalve DSA 3217/16px* pressure measurement arrays. The *DSA* acquires around 100 samples per second which are automatically aver-

aged, yielding an effective sampling rate of 1Hz. These measurements allow us to recover the pressure distribution  $p(s)$  with  $s$  being the curvilinear abscissa and deduce the pressure coefficient  $C_p(s)$  distribution:

$$C_p(s) = \frac{p(s) - p_{ref}}{p(0) - p_{ref}}, \quad (1)$$

where  $p_{ref}$  is measured at the inlet of the wind tunnel test area and  $p(0)$ , the pressure measured at the head of the main cylinder. We denote by  $\overline{C_p}$  as the mean, and  $C_{p(\text{rms})}$  as the rms fluctuations of  $C_p(s)$ . The acquisition rate of *DSA* devices and the tubing length act as low-pass filters of the pressure on the body surface. Thus, the measured pressure fluctuations can only be used as an indicator of the real fluctuations since its magnitude might be very different from the true fluctuations. Similar to [13], we will use the base pressure which is a sensitive quantity regarding the wake flow modifications. It is computed from the spatial average of the 5 pressure taps that are distributed on the blunt base of the cylinder:

$$C_{pb} = \frac{1}{D} \int_{base} C_p(s) ds. \quad (2)$$

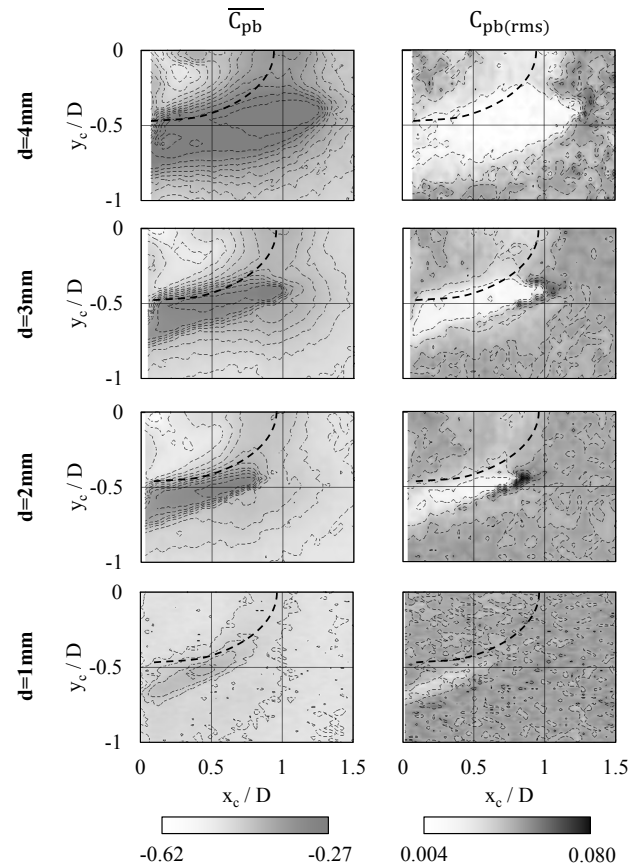
Particle Image Velocimetry is used to obtain the velocity field in the wake. The PIV system comprises a *Litron LP4550*, dual pulse 200mJ Nd:YAG laser, and a *Lavision Imager PRO* camera with a resolution of  $1600 \times 1400$  pixels. The setup acquires images at a rate of 11Hz, and *Lavision DaVis 7* software has been used to calculate the velocity fields. The vector calculation is done using single-pass, dual-frame cross-correlation on a constant window size. The interrogation window size is  $32 \times 32$  pixels. The final spatial resolution of the velocity fields is  $0.02D$ . Each acquisition records 500 image pairs, on which statistical analyses are performed.

Finally, to perform long time statistics, we use a single hot-wire placed on the symmetry axis of the geometry at  $x = 1.7D$ ,  $y = 0$ . It is oriented in such a way to be sensitive to the modulus of velocity  $xy$  plane. For each studied flow configuration, determined by the position of the control cylinder ranging from  $y_c/D = -0.48$  to  $y_c/D = -0.52$  in steps of  $0.004D$ , the velocity signal is acquired during 4 hours at a sampling rate of  $2\text{kHz}$ . The hot-wire sensor and *DISA 55* anemometer are manufactured by *DANTEC*. Since the hot-wire cannot discern between the stream-wise and cross-stream velocity components, we will use the modulus of velocity in  $xy$  plane for both PIV and hot-wire measurements, denoted as  $u_{xy}(t)$  for the instantaneous values, and  $U_{xy}$  for mean values.

### 3 Results

The sensitivity of the global properties of a turbulent wake behind a "D" shaped bluff body has been explored in detail in [10,11]. When a small circular control cylinder is inserted in the wake, the interaction between the free (separated) shear layers and the disturbance can yield a significant change of the global vortex shedding frequency and mean pressure drag. These changes are the result of the modification of the shear layer's thickness (therefore entrainment capacity) due to the presence of the control cylinder. The shear layer can either be thinned or re-laminarized if the control cylinder is placed on the low velocity side (of the shear), or it can be destabilized and more turbulent if the control cylinder is placed on the high velocity side, close enough so that the wake of the control cylinder influences the shear layer. In the previous publications, these effects were mainly considered with respect to mean values of drag and vortex shedding frequency as the global properties of the wake. However, the detailed mapping of the wake sensitivity also showed that some locations of the control cylinder cause a large increase in the fluctuations of drag.

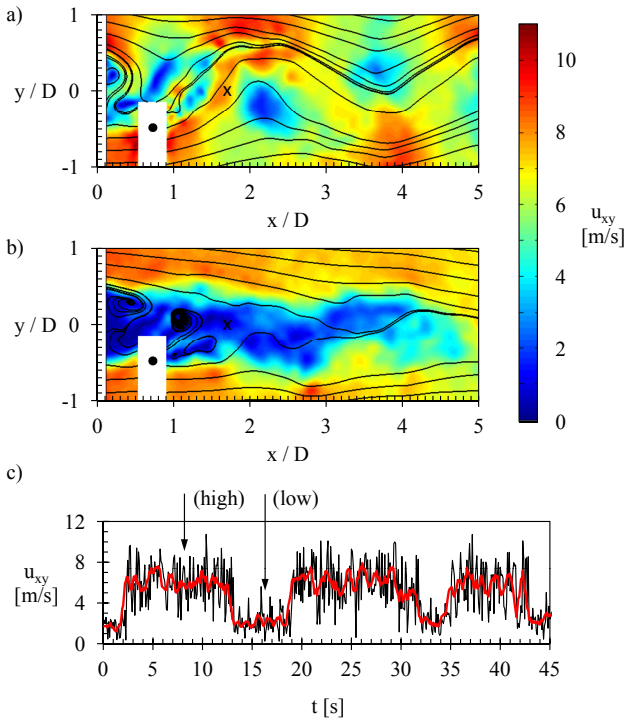
Figure 2 represents sensitivity maps of (left) mean base pressure  $\overline{C_{pb}}(x_c, y_c)$  and (right) base pressure fluctuations  $C_{pb(rms)}(x_c, y_c)$  for different sizes of the control cylinder. The base pressure is considerably increased, up to  $\overline{C_{pb}} = -0.27$  in a region that roughly corresponds to the mean location of the free shear layers. In [10,11], the high base pressure is related to an increase of the recirculation bubble which consequently shifts downstream the coherent fluctuations due to the shedding frequency of the Kármán vortices (the global mode). As a result, the body is surrounded by a quasi-steady flow and the fluctuation levels are lowest, as shown in the corresponding maps in the right column in figure 2. However, around the edges of the low pressure fluctuation region, we can observe small patches of very large base pressure fluctuations. This is clearly visible as black patches in the sensitivity maps for the 3mm and 2mm control cylinders. For the smaller control cylinder of 1mm these fluctuation crisis are absent. In that case, the control cylinder is smaller than the size of the shear layer thickness at separation, leading only to weak base-flow modifications. The fluctuations are not very pronounced for the 4mm control cylinder either. In this case, the control cylinder is too big in comparison to the local vorticity thickness of the shear layer, and the flow is constrained to one side of the control cylinder. This study will focus on the example of the 3mm control cylinder and the narrow regions of the fluctuations crisis, which are well defined in this case. We choose



**Fig. 2** Sensitivity maps of (left) base pressure  $\overline{C_{pb}}(x_c, y_c)$ , and (right) base pressure fluctuations  $C_{pb(rms)}(x_c, y_c)$ , for different sizes of the control cylinder. The dashed line in each map depicts a mean recirculation bubble size and shape for the natural flow.

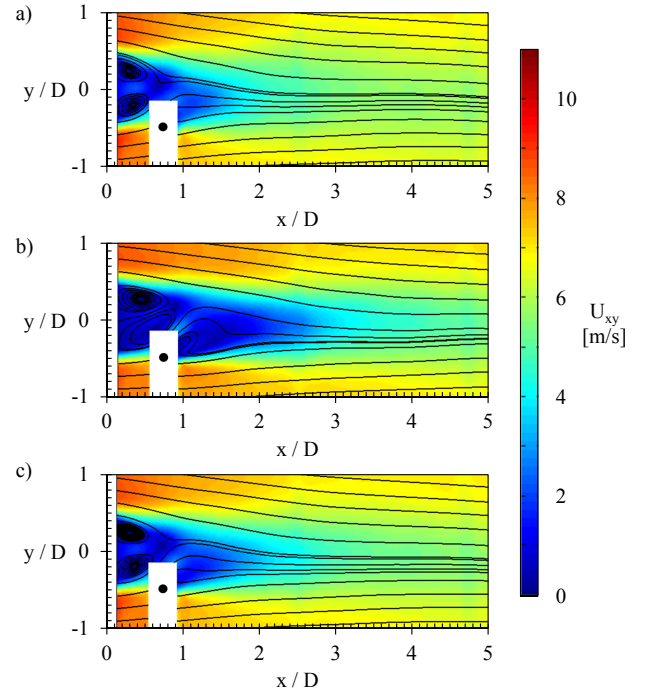
a fixed stream-wise location at  $x_c/D = 0.74$ , and test different vertical positions for the control cylinder, in the range  $-0.48 < y_c/D < -0.52$ . In figure 2(right), for the 3mm control cylinder, we can see that this interval of vertical positions places the control cylinder in the regions of low fluctuations, close the wake's center ( $y_c/D \rightarrow -0.48$ ), natural levels of pressure fluctuations ( $y_c/D \rightarrow -0.52$ ), and very high fluctuation levels in the middle, around  $y_c/D = -0.5$ .

Figure 3(a-b) shows two instantaneous velocity fields obtained from a PIV acquisition at 11Hz when the control cylinder is positioned at  $x_c/D = 0.74$ ,  $y_c/D = -0.50$ , which corresponds to the middle of the critical region. The two snapshots are drastically different although the control cylinder is in the same position. The velocity field in figure 3(a) shows a very small low velocity region at the base of the bluff body and a well-defined trace of vortex street further downstream. Figure 3(b) exhibits a huge region of slow fluid motion and no observable vortex shedding. In this case shedding is delayed to a downstream location approximately equal



**Fig. 3** Instantaneous PIV measurements of velocity  $u_{xy}$  and streamlines for the bi-stable flow, when the control cylinder is placed at  $x_c/D = 0.74$ ,  $y_c/D = -0.50$ . Instantaneous velocity fields represent a) small, and b) large recirculation bubble states, corresponding to high and low wake speeds, respectively. c) Time series of the modulus of velocity in the wake, measured from the ensemble of PIV snapshots at  $x/D = 1.7$ ,  $y/D = 0$  (marked with "x"). Positions (High) and (Low) correspond to snapshots shown in (a) and (b), respectively. Black line denotes instantaneous data  $u_{xy}$  and the red line represents a simple moving average over a time window of  $0.6s$   $U_{xy(SMA)}$ .

to around 4 – 5 diameters of the main body. These two instantaneous velocity fields are representative of the two states of the bi-stable wake flow regime. In further text, we will refer to the case of the small recirculation region and high wake velocity (figure 3a) as the "high" state and the case of the large recirculation region and low wake velocity as the "low" state. Figure 3(c) shows time series extracted from the PIV acquisition of modulus of velocity  $u_{xy}(t)$  measured at  $(x = 1.7D, y = 0)$ . This location is a relevant indicator of the flow states. The time series present temporal variation of about few seconds, very large compared to that of the vortex shedding period ( $1/f_0 = 14.3ms$ ). Most of the time, the local velocity has two mean values of around  $7m.s^{-1}$  and  $2m.s^{-1}$ . The simple moving average of velocity is used to construct conditional averaging of the PIV snapshots in order to visualize the mean velocity fields for the two states. Figure 4 shows the average of the ensemble of snapshots for (a)  $U_{xy(SMA)} > 4m.s^{-1}$  and (b)



**Fig. 4** Conditional averaging of PIV snapshots: a) high state, b) low state, c) average of the entire ensemble.

$U_{xy(SMA)} < 4m.s^{-1}$ , while the average of the entire ensemble is shown in (c) for comparison. These mean flows are relevant to the two instantaneous flow states observed in figure 3(a–b). The high state wake shows that the free shear layer, closest to the control cylinder, is undergoing a roll-up immediately behind the base of the main body, as if completely ignoring the presence of the control cylinder. Conversely, the main characteristic of the low state is that the control cylinder is at the limit between high velocity outer flow and low velocity recirculation bubble, indicative of a re-attachment of the free shear layer to the small control cylinder [11].

As shown in figure 3(c), the state switching appears to occur on relatively long time scales. In order to explore the dynamics of the switching, a long duration (4h), high sampling rate (2kHz) acquisition is performed using a hot-wire sensor. The hot-wire is placed at  $x = 1.7D$ ,  $y_c = 0$  (identical to the point data from PIV shown in figure 3c), and the acquisitions are performed for control cylinder placed horizontally at  $x = 0.74D$  and vertically through a range of  $-0.48 < y_c/D < -0.52$ . This means that the whole vertical size of the region of interest is only  $0.04D$  or 1mm in length. It is explored using 11 positions of the control cylinder, with 0.1mm as an in-between step.

The impact of the position of the control cylinder is first estimated using the Probability Density Functions (PDFs) of instantaneous velocity, shown in figure 5(a).

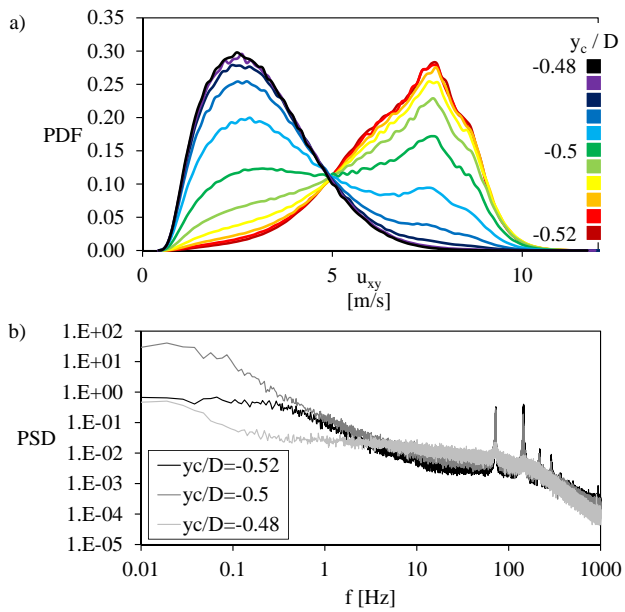


**Fig. 5** a) PDF of the stream-wise velocity  $u_{xy}(t)$  measured with a hot-wire placed at  $x = 1.7D$ ,  $y = 0$ . Each curve corresponds to a vertical position of the control cylinder from  $y_c/D = -0.48$  to  $y_c/D = -0.52$ . b) Velocity spectra from the hot-wire measurements for the two extreme positions and the middle position of the control cylinder.

Each curve corresponds to one position of the control cylinder  $y_c/D$ . For values towards the wake center, the velocity PDFs present a maximum around  $u_{xy} = 2.5\text{m}\cdot\text{s}^{-1}$ , while this maximum is around  $7.5\text{m}\cdot\text{s}^{-1}$  for control cylinder positions towards the wake limit. These PDFs clearly evidence the asymmetry of the high and low states, from their shape around the mode as well as from the level of their tails.

Figure 5(b) presents three velocity power density spectra obtained for three positions of the control cylinder. The spectra have common features: well defined peaks associated to the vortex shedding at  $f \simeq 72\text{Hz}$ , an inertial range starting for higher frequencies and a plateau at very low frequencies. An exception is the position  $y_c/D = -0.48$ , where the amplitude at the vortex shedding frequency is significantly reduced. This corresponds to the stream-wise displacement of the global mode, i.e. a large recirculation bubble. In the 0.1Hz-50Hz frequency range, the three spectra slightly differ the one from the other. The one obtained for  $y_c/D = -0.50$  and corresponding to the highest  $C_{p(\text{rms})}$  value, develops a close to  $-2$  slope over all this frequency range. This behavior is still visible, even if weaker, for  $y_c/D = -0.52$  for which the bi-stability is much less important, but it vanishes for  $y_c/D = -0.48$ .

A sample (500s) of the recorded hot-wire velocity signal for the control cylinder at  $y_c/D = -0.5$  is shown in

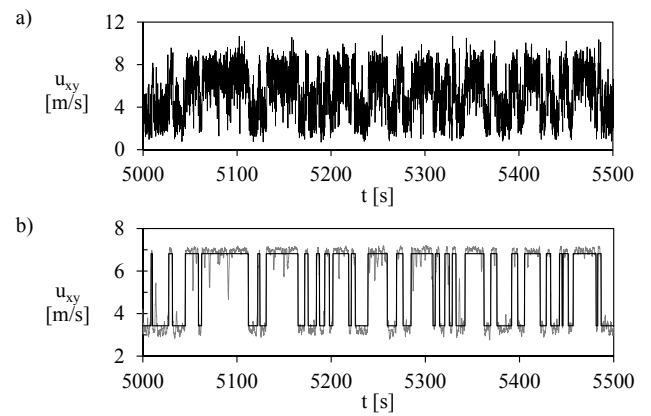


**Fig. 6** Time series of 500 seconds of the modulus of velocity  $u_{xy}$  from the hot-wire, with the two flow regimes visible; a) raw signal, b) simple moving average applied to the velocity signal, performed over 2000 samples and the associated binarization (black line) of the velocity signal used for detection of the flow state.

figure 6(a); the two states are clearly observable with a much better temporal resolution. In order to isolate each state, we have performed a moving average of the signal over 2000 points corresponding to 1 s as shown on figure 6(b). The average signal shows more clearly the switches between the two states. This signal is binarized by associating to high (resp. low) state portions of the signal with velocity higher (resp. lower) than  $5\text{m}\cdot\text{s}^{-1}$ . Averages in the high and low state are then calculated on this raw binary signal. The signal is then further binarized by assuming that it actually switches from one state to a new one if: (i) it crosses the  $5\text{m}\cdot\text{s}^{-1}$  threshold and (ii) it crosses the average value of the new state. This refinements allowed us to get rid of the excursions as the one observed before  $t = 5100$  s in figure 6(b).

We turn now to the statistical analysis of the switches between the two states. For the purpose, we consider the realization to observe either the high state or the low state during the sampling time interval  $dt$ . The observed states are directly given by figure 6(b) as a function of time after the velocity signal has been binarized. The fraction of time spent in the high state  $T_S^+/T$ , respectively in the low state  $T_S^-/T$ , is simply given by the number of observations of high state  $N^+$ , respectively low state  $N^-$  during the  $N$  realizations corresponding to the total duration of the acquisition  $N \times dt = T = 4\text{h}$ . Both fractions of time spent are displayed in figure 7(a), as a function of the control cylinder position. The fractions are equal near, but not exactly  $y_c/D = -0.5$ , which confirms the asymmetry observed earlier in the instantaneous velocity PDFs (figure 5a).

By counting the number of transitions between both states (indifferently from high to low or from low to

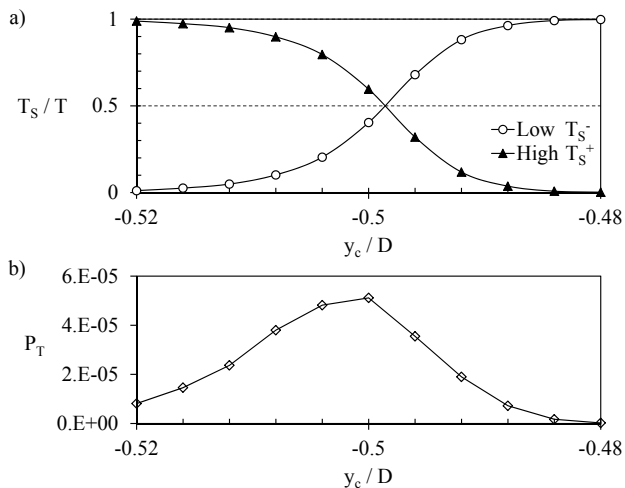


**Fig. 7** Statistics of binarized velocity data: a) fraction of time spent in low state  $T_S^-$  (circles) and high state  $T_S^+$  (triangles), and b) the probability of switching between flow states, as a function of the control cylinder position.

high), we assess to the probability  $P_T$  of the wake to switch states during the time interval  $dt$ , i.e. during one realization. This probability is plotted in figure 7(b), and is at a maximum when the wake explores the two states in equal proportion. We now consider the event of observing  $k$  consecutive same states, where  $k$  is related to the time spent  $T_S = kdt$  in one state (indifferently high or low). The experimental statistics of  $k$  are shown in figure 8. We can model these statistics by assuming that the realizations are independent. In that case, the probability to observe  $k$  consecutive same states is associated to  $k$  realizations having each a probability  $1 - P_T$  to not be a transition, and a last realization having a probability  $P_T$  to make a transition. This simple model predicts a statistics for  $k$ :

$$P(k) = P_T(1 - P_T)^k, \quad (3)$$

that satisfactorily superimposes on the experimental data (there is no fit). Therefore, we can conclude that the dynamics of flow re-attachment are fully associated with a random process. For the position  $y_c/D = -0.5$  which corresponds to the highest probability to switch states, the mean time spent is the shortest of all the positions of the control cylinder, and is  $\langle T_S \rangle = dt/P_T \approx 10$ s. These long time dynamics occur on periods of two to three orders of magnitude longer than the period for vortex shedding of the D-shape cylinder.

#### 4 Concluding remarks

The mapping of the wake of a bluff body has been presented for several different circular control cylinders.

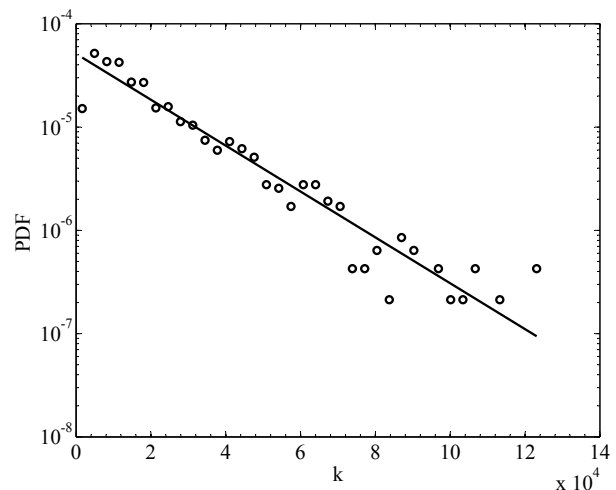


**Fig. 8** PDF of having  $k$  consecutive realizations with no transition (see text), the random variable  $T_s = kdt$  is the time spent in a same state.

It is observed that control cylinders whose diameter is large enough to cause mean flow modifications, can not only lead to damping, but also to large fluctuations of the aerodynamic forces acting on the main cylinder.

The damping effect originates from the displacement of the vortex shedding process downstream of the main cylinder, thus reducing the signature of the vortices on the base pressure. This occurs whenever the control cylinder is placed on the low speed side of either of the two shear layers, enabling the affected shear to attach to the control cylinder. Through attachment, the shear layer is re-laminarized and its roll-up and vortex creation are delayed downstream.

The increased fluctuations however, are a consequence of phenomena working on much longer time scales than the vortex shedding. These fluctuations are caused by intermittent attachment and detachment of the flow on and from the control cylinder. The differences in recirculation bubble size between the attached and detached flow states are very large, and so, the pressure at the base fluctuates between two very different values, which is observable in the base pressure fluctuations  $C_{p(rms)}$  sensitivity maps.

At the focal point of these high *rms* regions, the flow spends almost equal amounts of time in each of the two possible states. It is also shown that flow is more stable when the control cylinder is placed at the location which ensures flow attachment and a large recirculation bubble. In this state there are very few excursions into a high speed wake state, i.e. a small bubble. There is no observable pattern for choosing one state or the other, and we can conclude that the process is stochastic and invariant of its past history.

## References

1. A. Roshko, NACA TN (3169) (1954)
2. J. Gerrard, *Journal of Fluid Mechanics* **25**(02), 401 (1966)
3. M. Zdravkovich, *Flow around circular cylinders, vol. 2, Applications* (Oxford Univ. Press, New York, 2003)
4. M.M. Alam, H. Sakamoto, *Journal of fluids and structures* **20**(3), 425 (2005)
5. B.S. Carmo, J.R. Meneghini, S.J. Sherwin, *Physics of Fluids* **22**(5), 054101 (2010)
6. M.M. Alam, Y. Zhou, J. Zhao, O. Flamand, O. Boujard, *International Journal of Heat and Fluid Flow* **31**(4), 545 (2010)
7. A. Ekmecki, D. Rockwell, *Journal of Fluid Mechanics* **665**, 120 (2010)
8. H. Sakamoto, H. Haniu, K. Tan, *ASME Transactions Journal of Fluids Engineering* **113**, 183 (1991)
9. H. Sakamoto, H. Haniu, *Journal of fluids engineering* **116**(2), 221 (1994)
10. V. Parezanović, O. Cadot, *Physics of Fluids* **21**, 071701 (2009)
11. V. Parezanović, O. Cadot, *Journal of Fluid Mechanics* **693**, 115 (2012)
12. P. Strykowski, K. Sreenivasan, *Journal of Fluid Mechanics* **218**, 71 (1990)
13. A. Roshko, *Journal of Wind Engineering and Industrial Aerodynamics* **49**(1-3), 79 (1993)